energies

MDPI

Article

The Wideband Oscillatory Localization Method Based on Combining Compressed Sensing and Graph Attention Networks

Jinggeng Gao [1], Yong Yang [1], Honglei Xu [2], Yingzhou Xie [1], Chen Zhou [3,*] and Haiying Dong [3,*]

[1] State Grid Gansu Electric Power Research Institute, Lanzhou 730000, China; gao2541@163.com (J.G.); yy8801@126.com (Y.Y.); yingzhouxie@foxmail.com (Y.X.)
[2] State Grid Gansu Electric Power Company, Lanzhou 730000, China; angle_xhl@126.com
[3] School of New Energy and Power Engineering, Lanzhou Jiaotong University, Lanzhou 730070, China
* Correspondence: 11230951@stu.lzjtu.edu.cn (C.Z.); hydong@mail.lzjtu.cn (H.D.)

Abstract: Due to the increasing integration of new energy sources, the power system now exhibits low inertia, in which the broadband oscillation problem is increasingly significant in the face of the strong coupling of complex and variable power systems, and the current lack of uniform and effective mathematical models and analysis methods. To solve this major problem, a broadband oscillation localization method based on the combination of compressed perception and graph attention network (GAT) is proposed. The method firstly uses the principle of compression perception to compress and transmit the oscillation time series data of the sub-station, reconstructs the compressed signal at the master station and aggregates the grid topology and node characteristic information to effectively reduce the redundancy of the oscillation data; reconstruction error is only 0.031, takes into account the balance of the samples and the effectiveness of the computation, and adopts the multi-attention mechanism and the cross-entropy loss function to improve the performance of the model training. Finally, the offline training and online evaluation model based on the GAT algorithm is constructed, and the accuracy of the model is up to 98.5%; and the results show that the method has a high positioning accuracy and a certain anti-noise ability at the same time.

Keywords: power system; compressed sensing; graphical attention networks; wideband oscillation positioning

check for updates

Citation: Gao, J.; Yang, Y.; Xu, H.; Xie, Y.; Zhou, C.; Dong, H. The Wideband Oscillatory Localization Method Based on Combining Compressed Sensing and Graph Attention Networks. *Energies* **2024**, *17*, 6062. https://doi.org/10.3390/en17236062

Academic Editors: Kegong Fang, Gangli Zhu and Shenghua Liu

Received: 29 October 2024
Revised: 25 November 2024
Accepted: 26 November 2024
Published: 2 December 2024

Copyright: © 2024 by the authors. Licensee MDPI, Basel, Switzerland. This article is an open access article distributed under the terms and conditions of the Creative Commons Attribution (CC BY) license (https://creativecommons.org/licenses/by/4.0/).

1. Introduction

While the wide application of new clean energy sources such as photovoltaic and wind power promotes the clean and efficient utilization of energy, it also brings the challenges of reduced inertia and weakened anti-interference ability to the power system; in particular, the broadband oscillation problem is becoming more and more prominent. The stochastic nature of new energy output and the interaction between electronic devices can lead to machine-grid coupling oscillations, and the oscillations generated when large-scale new energy is connected to the grid show a broadband trend. For example, in 2015, sub/super synchronous oscillations occurred in direct-drive wind turbine clusters in the Hami area of Xinjiang, when they were connected to the weak AC grid [1]; 250~350 Hz occurred in the offshore wind power via flexible direct grid-connection project in the North Sea of Germany [2,3]; and medium- to high-frequency oscillations ranging from 500 to 1270 Hz occurred in China's Yunnan Lusi Flexible Transmission Project, Zhejiang Zhoushan Flexible Project, and Guangxi Muger Wind Farm, etc. [4,5]. Broadband oscillations not only lead to sharp fluctuations in voltage and frequency, but also cause a series of chain reactions, such as overloading of equipment and erroneous operation of protective devices, and may even lead to localized or large-scale power outages; so it is particularly important to accurately locate the point of its oscillations and quickly take suppression measures.

At present, the main domestic and international research methods on broadband oscillation are: eigenvalue analysis [6,7], impedance modelling [8], open-loop resonance [9] and so on. Eigenvalue analysis determines the stability of a system by calculating the eigenvalues of the system state matrix. Impedance modelling determines the stability of the system by analyzing the impedance characteristics of the system, and can be used to design controllers to change the impedance characteristics of the system in order to improve the stability of the system. Open-loop resonance identifies the intrinsic oscillatory modes of a system and their characteristics by performing tests under open-loop conditions and measuring the frequency response function of the system. Although this method is capable of describing the dynamic behavioral information of the oscillations in detail, it requires long computation time and therefore struggles to meet the demand for fast localization of the oscillation point [10].

Due to the limitation of the phasor measurement unit (PMU) device, there are fewer studies on the localization of the sub/hypersynchronous oscillation source in the literature [11,12]. By analyzing the harmonic currents between the grid points, the propagation mode of the sub/hypersynchronous oscillations can be deduced, which leads to the localization of the source of the oscillations. In the literature [13,14], on the other hand, studies are based on the relationship between the transient energy flow and the energy of sub/super synchronous oscillations, establishes their correlation with the damping characteristics, and explores the method of using the transient energy flow for identifying the source of forced oscillations. However, the above methods usually rely on mechanisms to model complex broadband oscillations which, coupled with the increasing size of the power system and the variable operating conditions, means that the localization methods based on certain assumptions may not be consistently effective. Therefore, these uncertainties and limitations need to be taken into account in practical applications.

In recent years, the development of artificial intelligence technology and the promotion and application of wide-area measurement system, through the "offline training, online evaluation" way, can quickly complete the node classification, load prediction, oscillation localization and other tasks [15–17]. Studies [18,19] have used compressed perception and a graph convolutional neural network to do a preliminary study of the wideband oscillation source localization problem, but did not consider the attention mechanism. Studies in the literature [20,21] have proposed a broadband oscillation wide-area localization method based on self-encoder signal compression and a long short-term memory (LSTM) network, using s self-encoder to compress and decode the information of each sub-station so as to carry out a wide-area monitoring and analysis of broadband oscillation signals. GAT [22–24], as a graph deep learning algorithm, is able to learn its own node feature information while weighting the aggregation of neighboring node states based on the grid topology feature matrix, due to its unique graph data reading capability and multi-head attention mechanism. The exploration results show that GAT can accurately identify the source of oscillations by utilizing the real-time data of nodes (e.g., generating stations, substations, and load points) in the power system, and dynamically capturing the complex interactions among the nodes through the attention mechanism. This not only improves the accuracy and speed of oscillation localization, but also provides strong support for real-time monitoring and early warning, which helps O and M personnel to take timely measures to ensure the stable operation of the power system.

In this paper, a broadband oscillatory localization model based on the GAT algorithm is developed. Section 2 mainly utilizes the principle of compressed sensing to compress the data sampling, Section 3.1 adopts the multi-head attention scheme to improve the evaluation performance of the GAT algorithm model, and Section 3.2 introduces the cross-entropy loss function to reduce the influence of different difficulty samples on the training convergence process, and builds up the oscillation localization model. Finally, in Section 3.3, the historical sample set is constructed for training to realize the transient stability identification of the power system under the new operation scenario, and the results verify the effectiveness of the method proposed in this paper.

2. Compression Method for Wideband Oscillating Signals

Nyquist's theorem shows that in order to make the digital signal after sampling retain as much as possible the characteristics of the original signal, the sampling frequency must be greater than two times the highest frequency of the signal; and in the face of broadband oscillation signals that may be as high as thousands of hertz, it is difficult to effectively monitor the broadband oscillation signals of the sub-station. Therefore, compression sensing of the data from the sub-station to be sampled and uploaded to the master station can be used as the node feature information to establish the mapping relationship.

2.1. Principle of Compressed Sensing

Compressive sensing (CS) [25] exploits signal sparsity to achieve sampling at frequencies far below those required by Nyquist's sampling theorem, which can solve the problem of wideband oscillatory data transmission under the existing bandwidth; and its sparse decomposition principle is shown in Figure 1.

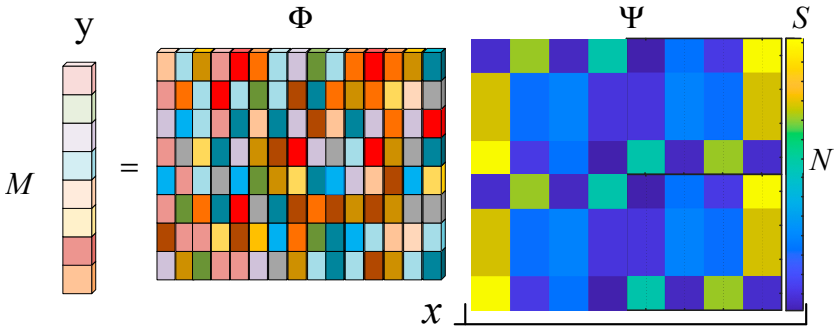

Figure 1. Compression-aware sparse decomposition principle.

For a signal $x \in \mathbb{R}^N$, the expression for obtaining a compressed signal y is:

$$y = \Phi x \tag{1}$$

where, $\Phi \in \mathbb{R}^{M \times N}$ is called the measurement matrix; $y = [y_1, y_2, \cdots, y_M]$ is the compressed signal of the dimension, where M is the compressed signal dimension and N is the original signal dimension, $M \leq N$. If it exhibits sparse properties under a certain transform domain:

$$x = \Psi S \tag{2}$$

where, $\Psi \in \mathbb{R}^{N \times N}$ is a sparse basis matrix; S is denoted as the projection of the signal onto the sparse domain and is called the sparse coefficient. If the original signal is sparse in the S-base (there are only K nonzero terms, where $K \leq N$), the expression for the observation model for compressed perception is obtained by combining Equations (1) and (2):

$$y = \Phi \Psi S = \Theta S \tag{3}$$

where, Θ is the perceptual matrix, since the dimension M of the compressed signal y is smaller than N, it is a difficult problem to obtain a sparse solution to the underdetermined Equation (3), so the problem of solving Equation (3) can be transformed into a L_1-paradigm minimization problem:

$$\min_{S} \parallel S \parallel_1 \ s.t. y = \Phi \Psi S \tag{4}$$

The Φ in the above equation must satisfy the finite equidistance property (RIP), and the signal can be accurately reconstructed from the M measurements using K non-zero coefficients. From the above equation, it can be seen that in order to achieve the compressed sampling and reconstruction of wideband oscillation wide-area signals, three parts are required:

(1) Design the sparse transform to find the proper basis to make the signal x sparse in the Ψ domain;
(2) Design the projection measurement matrix so that it satisfies the RIP criterion;
(3) The classical CS reconstruction algorithm is selected to perform signal recovery based on the a priori information of the selected measurement matrix Φ and sparse matrix Ψ. The signal recovery is performed by the classical CS reconstruction algorithm.

2.2. Wideband Oscillation Signal Compression Sensing and Reconstruction

For the monitoring of broadband oscillations in the grid, it is usually only necessary to observe the active power signals at each node. In order to be able to make up for the difficulty of effective sparse representation of Fourier sparse for instantaneous bursty signals, in this paper, we will use Gabor dictionary and Fourier dictionary cascade combined into an over-complete dictionary, to better adapt to the sparse representation needs of different types of signals. The Gabor atomic real number expression is:

$$g(t) = \frac{1}{\sqrt{\sigma\sqrt{\pi}}} e^{-\frac{t^2}{2\sigma^2}} \cos(2\pi f_0 t + \varphi) \tag{5}$$

where, $g(t)$ is the Gabor atom, σ is the standard deviation of the Gaussian window, which controls the width of the window, f_0 is the frequency modulation factor, and φ is the phase parameter.

$$\Psi_H = [\Psi_G, \Psi_F] \tag{6}$$

where, Ψ_G is the Gabor sparse dictionary and Ψ_F is the Fourier sparse dictionary, which can be obtained using the following equation:

$$\Psi_F = fft\left\{ \begin{pmatrix} 1 & \cdots & 0 \\ \vdots & \ddots & \vdots \\ 0 & \cdots & 1 \end{pmatrix}_{N \times N} \right\} / \sqrt{N} \tag{7}$$

The broadband oscillation data within the wth measurement window can be sparsely represented using an overcomplete synthetic dictionary as:

$$X^{T_w} = \psi_H \cdot S_i^{T_w} \tag{8}$$

where $S_i^{T_w}$ is the sparsity coefficient of the broadband oscillation data in the its node corresponding to the w time window, and the original data can be recovered by a linear combination of the sparse sparsity and the atomic parameters of the corresponding column.

The projection measurement matrix is the main purpose of mapping a high dimensional signal into a low dimensional space while preserving the key information of the signal. The construction methods are mainly divided into random observation matrix and deterministic observation matrix; in this paper, we use a Gaussian matrix as the measurement matrix, the dimension of matrix Φ is $M \times N$. Each element in the matrix obeys a Gaussian distribution with variance $1/\sqrt{M}$. The matrix is a Gaussian distribution with variance c.

The reconstruction algorithms are Basis Pursuit (BP), Orthogonal Matching Pursuit (OMP), Matching Pursuit (MP), CoSaMP (Compressed Sampling Matching Pursuit), and Iterative Soft Thresholding Algorithm (ISTA) [26]; of which, the CoSaMP algorithm is an improvement of the OMP algorithm by introducing more efficient atom selection and removal mechanisms, as well as better resistance to noise, which gives it a significant advantage over OMP in the sparse signal recovery task. The CoSaMP algorithm is particularly suited for processing noisy data and high-dimensional data. The specific steps are shown in Algorithm 1.

Algorithm 1: CoSaMP Algorithm Signal Reconstruction Steps

Input

- Perceptual matrix $\Theta = \Phi\Psi$ of $M \times N$
- dimensional compressed signal x
- Signal Sparsity K

Output

- Signal sparse representation coefficient estimation S
- $N \times 1-$dimensional residual $r_n = y - \Theta_n S_n$

Procedure

(1) Initialize $r_0 = y$, $\Lambda_0 = \varnothing$, $\Theta_0 = \varnothing$, $t = 1$;
(2) Calculate $u = abs\left[\Theta^T r_{t-1}\right]$, choose the 2K largest values in u, and form the set J_0 by taking the Θ columns corresponding to that value and numbering them j;
(3) Let $\Lambda_t = \Lambda_{t-1} \cup J_0$, $\Theta_t = \Theta_{t-1} \cup a_j$;
(4) Find the least squares solution for $y = \Theta_t S_t$;
(5) Select the K item with the largest absolute value from S_t as S_{tK}, the corresponding K column in Θ_t as Θ_{tK}, and the corresponding Λ_t column number as Λ_{tK}, update the set $\Lambda_t = \Lambda_{tK}$;
(6) Update residuals $r_t = y - \Theta_{tK} S_{tK} = y - \Theta_{tK}\left(\Theta_{tK}^T \Theta_{tK}\right)^{-1} \Theta_{tK}^T y$;
(7) $t = t + 1$, when $t \leq n$, return to step 2 to continue iteration, if $t > n$ or residual r_t reaches the target then stop iteration;
(8) The reconstruction yields that S has nonzero terms at Λ_{tK}, whose values are the S_{tK} of the last iteration, respectively;
(9) After obtaining S, the signal $x = \Psi S$ can be reconstructed using the sparse matrix.

In Algorithm 1, r_t denotes the residuals, t denotes the number of iterations, $\varnothing$ is the empty set, J_0 denotes the number of columns found in each iteration, Λ_t denotes the set of columns in the first iteration, a_j denotes the first column of the matrix Θ, and $abs[\,]$ denotes the modulus value.

Constructed by 10 Hz, 50 Hz, 200 Hz, and 400 Hz superimposed on the wideband oscillation of the original signal—as shown in Figure 2—setting the sampling frequency for $f_s = 800$ HZ, the data segment length $N = 260$, CS compression multiples of $m = 4$ (for an original oscillation data segment after CS compression there are only $M = N/n = 65$ under sampled signals, as shown in Figure 3) significantly improves the efficiency of data transmission. By using the OMP algorithm to reconstruct the compressed 65 data points, as shown in Figure 4, the reconstructed waveform and the original data waveform error is small, as shown in Figure 5; which proves the effectiveness of the proposed method, and also shows that a small number of compressed data points are specific to the key features of the original signal, which can be used directly as the input value of the feature matrix to achieve the localization of the wideband oscillator source in the deep-learning network.

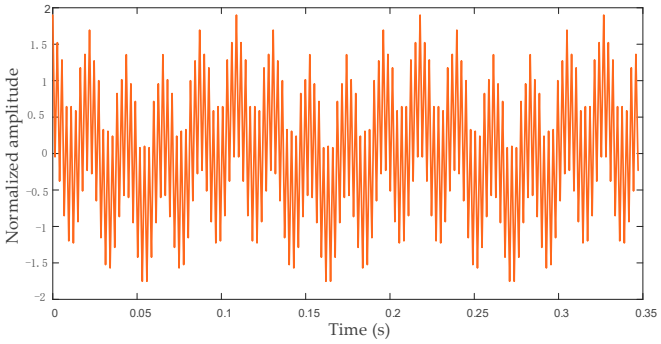

Figure 2. Raw oscillating signal.

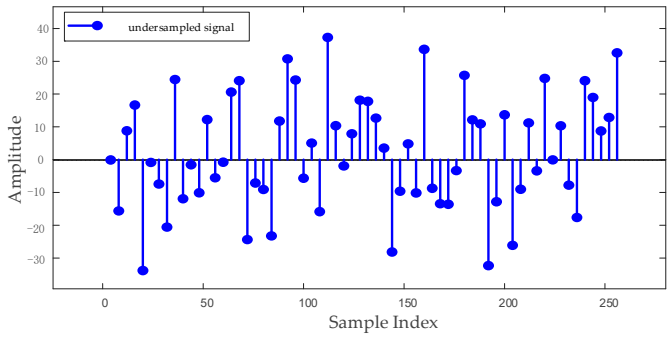

Figure 3. Compression of discrete signals.

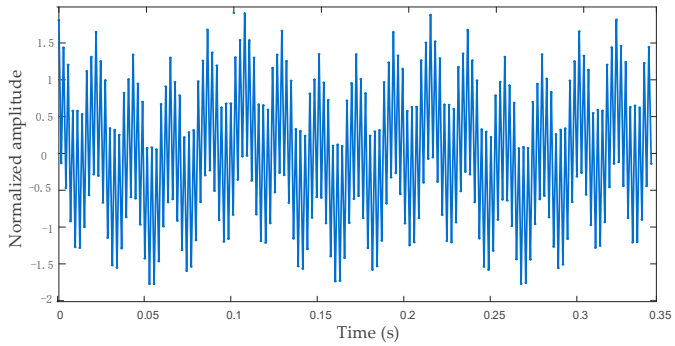

Figure 4. Reconstructed signals.

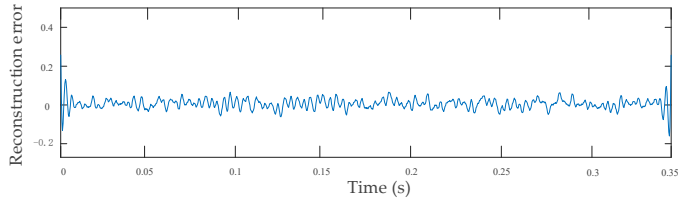

Figure 5. Reconstruction error.

The compressed perception technique can effectively downscale the high-dimensional broadband oscillatory signals, reducing data redundancy and storage requirements. This not only helps the efficient learning of the graph neural network, but also enables the model to run under lower computational resources, which improves the overall computational efficiency; and the low-dimensional signal processed by compressed perception can be reconstructed back to the original high-dimensional signal with high accuracy. The low-dimensional data can well retain the key features and information of the original signal, ensuring the accuracy of the subsequent analysis.

3. GAT-Based Wideband Oscillation Localization Method

The power system is a high-dimensional nonlinear system; when the system faces oscillation, it is necessary to quickly locate the oscillation node or region to effectively control the further evolution of the fault. The GAT algorithm is a deep-learning method for graph-structured data. It is mainly used to deal with datasets with complex relationships between nodes. GAT improves the traditional graph neural network (GNN) by introducing an attention mechanism that allows it to capture the dependencies between nodes more flexibly. the GAT algorithm proposed in this paper constructs a broadband oscillation localization model to be trained offline through the historical data samples, and evaluated online on the node information of the real-time monitoring, so as to judge the stable state of each node of the system after the perturbation, to realize the oscillation of the region.

3.1. GAT Multiple Attention Mechanism

The multi-head attention mechanism is similar to the multi-channel of the convolutional neural network; due to the complexity of its grid topology changes, in order to extract different node information, the multi-head attention mechanism helps capture complex relationships between nodes in the graph. Firstly, the calculation of the attention coefficient needs to be carried out, and the expression is:

$$\alpha_{ij} = \frac{exp(LeakyReLu(\vec{a}^T \left[W\vec{h_i} \parallel W\vec{h_j} \right]))}{\sum_{K \in N_i} exp(LeakyReLu(\vec{a}^T \left[W\vec{h_i} \parallel W\vec{h_k} \right]))} \tag{9}$$

where a_{ij} is the normalized attention weight, $\vec{a}$ is the vector to be learned, h_i is the input node attribute information, and $||$ is the stitching of the feature matrix.

A weighted summation of the attention coefficients a_{ij} computes new features that incorporate information about their neighborhoods:

$$h_{i+1,j} = \sigma\left(\sum_{j \in N_i} \alpha_{ij} W\vec{h_{i,j}} \right) \tag{10}$$

where: $h_{i+1,j}$ is the new node feature; σ is the activation function; j in $j \in N_i$ denotes all nodes neighboring i.

For each GAT a set of W and a matrices with different parameters are used, called an attention head; and to aggregate multiple attention heads, there are 2 ways of processing.

Averaging:

$$h_i'(k) = \sigma\left(\frac{1}{k} \sum_{k=1}^{k} \sum_{j \in N_i} \alpha_{ij}^k W^k h_j \right) \tag{11}$$

Splicing method:

$$h_i'(k) = \Big\Vert_{k=1}^{k} \sigma\left(\sum_{j \in N_i} \alpha_{ij}^k W^k h_j \right) \tag{12}$$

Figure 6 shows the type of multi-head attention aggregation process; this paper samples a three-head attention mechanism, and nodes of each attention coefficient are calculated independently of each other.

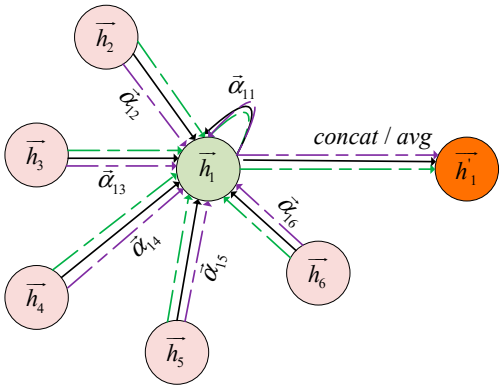

Figure 6. Multi-attention aggregation.

3.2. Broadband Oscillation Localization Model

In order to improve the accuracy of broadband oscillation localization, it is necessary to consider the temporal and spatial distribution characteristics focusing on the input characteristics and the temporal variability. In terms of temporal characteristics, the broadband oscillation phenomenon in the power system is affected by a variety of factors. In

this paper, the active power timing information P of nodes is proposed to be used as the input feature; in terms of the spatial characteristics of oscillation, the neighbor matrix A of the power network topology is input into GAT as the spatial information. In this way, the spatio-temporal data of the power system can be fully utilized to achieve accurate oscillation localization.

$$P = \begin{pmatrix} p_{1,1} & \cdots & p_{1,n} \\ \vdots & p_{t,n} & \vdots \\ p_{k+1,1} & \cdots & p_{k+1,n} \end{pmatrix} \tag{13}$$

$$A = \begin{pmatrix} a_{11} & \cdots & a_{1n} \\ \vdots & \ddots & \vdots \\ a_{n1} & \cdots & a_{nn} \end{pmatrix} \tag{14}$$

where P denotes the node electrical signals, respectively, n represents the number of nodes, and the elements of matrix A denote the connectivity between the nodes. A 1 represents that two nodes are connected and a 0 represents that two nodes are not connected.

By learning the mapping relationship between the oscillating node position labels and the feature matrix P, the trained GAT model—i.e., the broadband oscillation disturbance source localization model—can be obtained, denoted as:

$$\hat{S} = H_{GAT}(Y) = H_{GAT}(G(X_{in})) \tag{15}$$

where: $\hat{s}$ is the position label of the oscillation source; $H_{GAT}(\cdot)$ is the mapping function between the position label of the oscillation source and the feature matrix Y; $G(\hat{X_{in}})$ is the relationship function between the actual system volume measurement X_{in} and the feature matrix Y, which corresponds to the compression sensing process.

In practice, most of the sample labels are stable in the building of the dataset, which makes the positive and negative samples unbalanced, and more attention needs to be given to the oscillating samples; so, in this paper, we refer to the processing technique of transient stable identification of neighborhoods, and introduce the cross-entropy loss function with weights [27] to balance the samples:

$$loss(p) = -\frac{1}{M}\sum_{k=1}^{M}(w_0 y_{k,0}\ln(p_{k,0}) + \cdots + w_n y_{k,n}\ln(p_{k,n})) \tag{16}$$

where: $n = 3$ is the label value; M is the number of samples; $y_{k,0}$ and $y_{k,n}$ are the labels belonging to 0, 1, 2, and 3 in a sample, which are Boolean values; $p_{k,0}$ and $p_{k,n}$ are the probability values of the samples belonging to the various types of labels given by the discriminator in the range of [0, 1]; w_0 is the weight of the samples under the stable condition; and w_n is the weight of the samples labeled with n case.

The overall structure of the GAT-based wideband oscillation localization model is shown in Figure 7, with four layers. The data layer is the graph feature matrix A of the power system topological connection relationship and the perturbation sampling node information P, in the information learning layer by the multi-attention mechanism of the GAT to obtain more characteristics of the spatial and temporal information; in the all-connectivity layer, the use of the newly extracted node power feature information for classification, and based on the classification threshold in the output layer to output the localization area results.

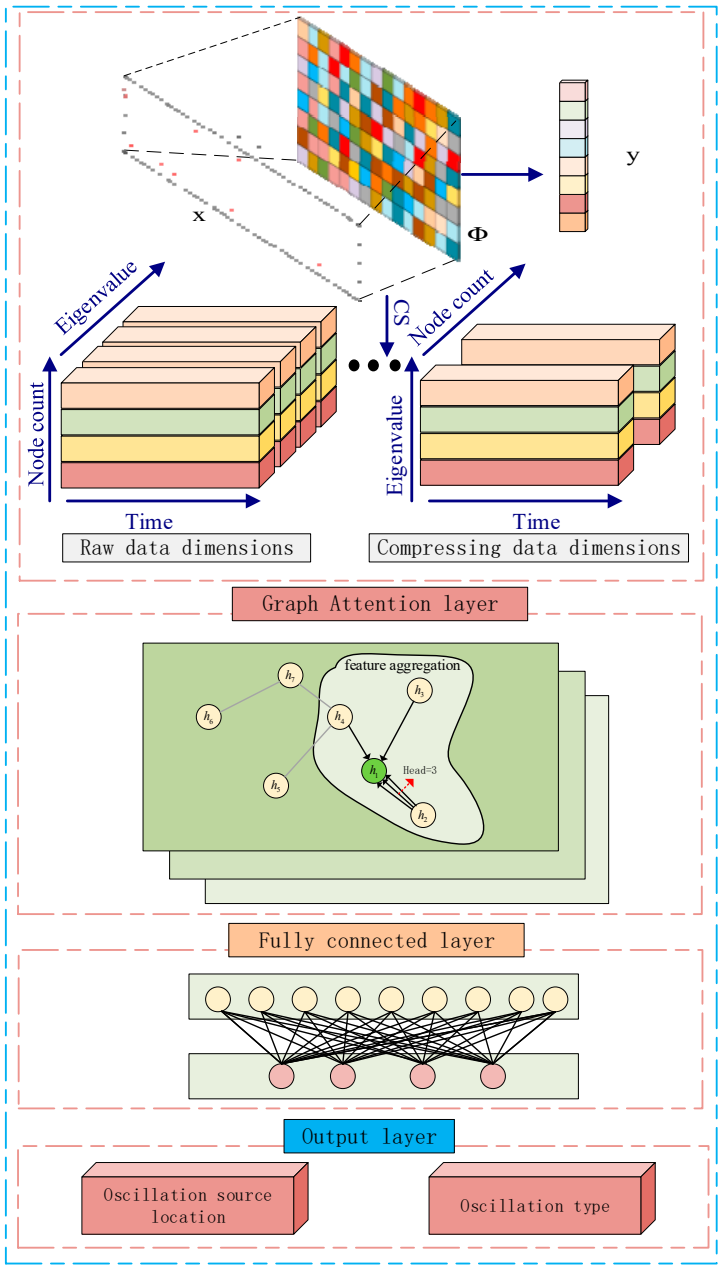

Figure 7. The broadband oscillatory localization model structure of GAT.

The dimensionality reduction of the input feature dimension after each layer of the broadband oscillation localization model can map the extraction process of the oscillation feature values, and provide some reference for adjusting the model structure. The model design in this paper adopts a four-layer dimensionality reduction structure. The first three layers are GAT layers, which realize the feature aggregation and extraction of the topological connection relationship of the grid, and the last layer is the fully connected layer (FC), which realizes the whole process, from obtaining feature information to oscillation localization.

3.3. Implementation of Oscillatory Source Localization Based on Compressed Sensing Combined with GAT

According to the broadband oscillation localization model proposed in Section 2.2, the specific flow of the broadband oscillation localization method implemented in this paper

based on compressed sensing and GAT algorithm is shown in Figure 8, in which the offline training steps are as follows:

(1) Simulation data generation. The PSASP simulation software is utilized to set different frequency perturbations and model control parameters on the improved IEEE-39 buses to make it undergo broadband oscillations, and to extract the diverse simulation data generated under different scenarios.
(2) Data compression. Low-dimensional signal data characterizing the current state is obtained by compressing the simulation data according to the CS principle, and categorical data labels are added sequentially.
(3) Selection of feature inputs. Select the input features of the broadband oscillatory localization model from the labeled simulation data and set up the training set, validation set, and test set according to 6:2:2.
(4) Offline training. A collection of training samples is input into the oscillatory localization model, and the feature data embedded in the input samples are fully learned by the model.

In addition, the following steps are applied for online assessment of power system transients:

(1) The PMU measurement tool is used to detect the dynamic data of each node in the sub-station in real time, and compress and upload them to the main station; and extract the transient stability determination-related feature information.
(2) The compressed relevant feature information of each sub-station is packed and fed into the trained broadband oscillation localization model for state determination.
(3) According to the broadband oscillation model's output judgment results, decide whether to use the appropriate measures, such as if the results of the judgment for the stability of the data only need to continue to monitor the rolling, if there is oscillation, to take measures to prevent further expansion of the fault.

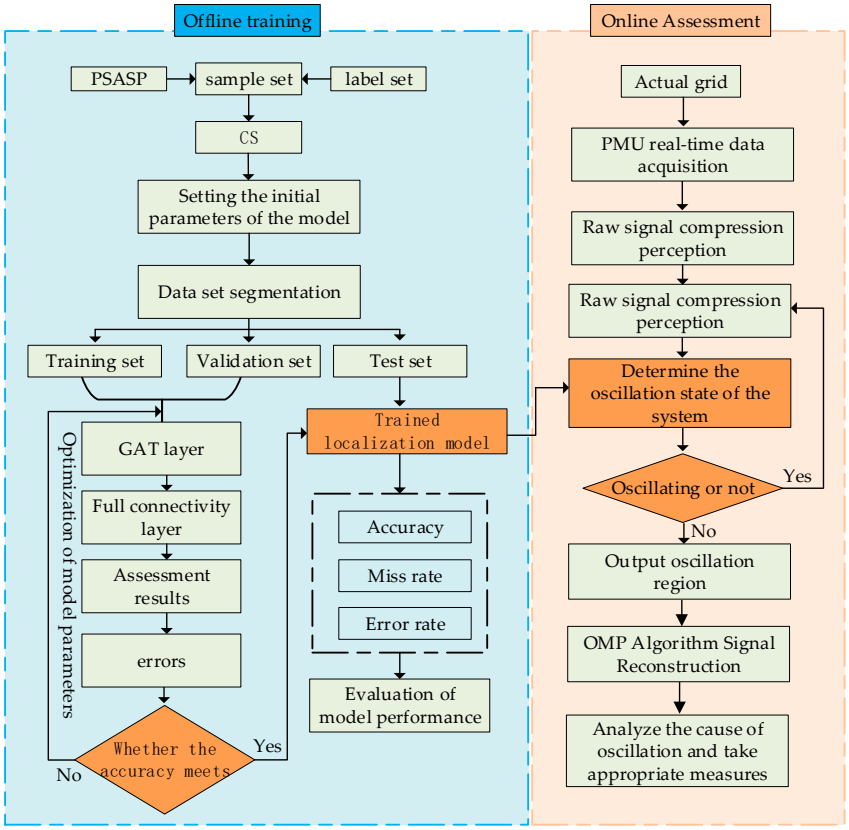

Figure 8. Broadband oscillation localization process framework.

4. Calculus Analysis

In this paper, we use the improved IEEE-39 buses system data as the object to verify the performance of the wideband oscillation localization model, and the arithmetic platform allotment is: Inter Core i7-11700 CPU 2.5 GHz/32 GB RAM, NVIDIA GTX 1660 SUPER GPU; and the CUDA architecture is utilized to make the parallel computation of the GPU and the CPU to improve the training speed. GAT is built based on Pytorch 3.6 learning framework.

The IEEE-39 buses built with PSASP simulation software are shown in Figure 9. Among them, node 37 is changed to a 300 MW doubly fed wind farm, and node 34 is changed to a 300 MW PV plant. The base power of the system is set to 100 MVA, the rated frequency is 50 Hz, and the generator is modeled by the classical second-order model.

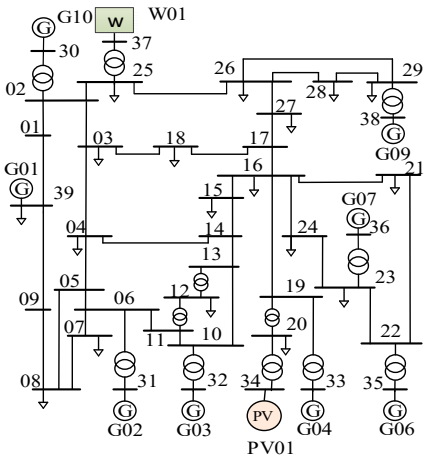

Figure 9. Improvements to the IEEE-39 buses system.

In order to fully equalize the training effect of the model, the perturbation settings involve the whole network as much as possible, to diversify the sample types. The setup system injects periodic perturbation signals with frequency (10∼40 Hz, 70∼100 Hz, 130∼160 Hz) at the prime mover of the generator, the grid side of the wind generator, and the grid side of the photovoltaic generator, respectively; and the load level is increased from 70% intervals of 5% to 115%, which constitutes the forced oscillation dataset.

The broadband oscillation sub-stations are compressed and sampled, and uploaded to the main station to form the graph sample; each graph sample contains 39 buses power data, each node after compression of the feature dimension constitutes the feature matrix p and the adjacency matrix A. A total of 3120 samples are generated based on the above conditions, and the above samples are classified into the training set, validation set, and test set according to the 6:2:2, where the training set is used for modeling. The training set is used for model optimization, the validation set is used to adjust the hyperparameters, and the test set is used to verify the generalization ability of the model.

4.1. Wideband Oscillation Data Compression Sampling

Due to the bandwidth limitation of the power system line transmission network, the main station is unable to comprehensively monitor the broadband oscillation signals, so the CoSaMP algorithm is used to monitor the broadband oscillation frequency bands and upload the low-dimensional compression data. Figure 10 demonstrates that the waveform of the 22 Hz sub-synchronous oscillation with the second and the third harmonics basically fits with the reconstructed waveforms, which indicates that the low-dimensional oscillation signal features extracted by compression perception can represent the original signals.

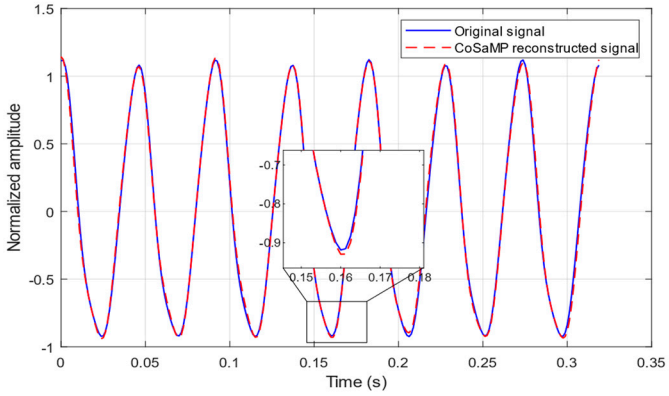

Figure 10. Comparison of original and CoSaMP reconstructed signals.

By comparing the waveforms of the CoSaMP algorithm and the OMP algorithm in different frequency bands, it can be clearly seen from Figure 11 that the reconstructed waveforms of the CoSaMP algorithm can be more closely matched to the original signals compared to the OMP algorithm, as shown in Table 1. By comparing the specific reconstruction time and error of the two algorithms, it can be observed that the reconstruction error shows a decreasing trend with the increase in the number of iterations of the CoSaMP algorithm; however, an increase in the number of iterations also leads to an increase in the reconstruction time. The increase in the number of iterations also leads to the prolongation of the reconstruction time. Therefore, in practical applications, it is necessary to find an optimal balance between the reconstruction accuracy and the computational efficiency to meet the requirements of the features.

Table 1. Compression-aware reconstruction error vs. time.

Compression-Aware Reconfiguration Methods	Epoch	Reconstruction Error (Normalized L2 Norm)	Reconfiguration Time/s
CoSaMP	50	0.06465830	30.394
	100	0.05457703	63.331
	200	0.03188598	107.565
OMP		0.26317165	33.137

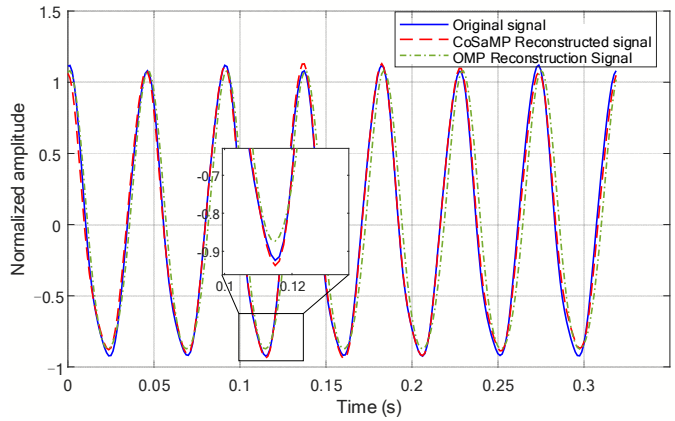

(**a**) 22 Hz sub-synchronous oscillatory oscillatory signal

Figure 11. *Cont.*

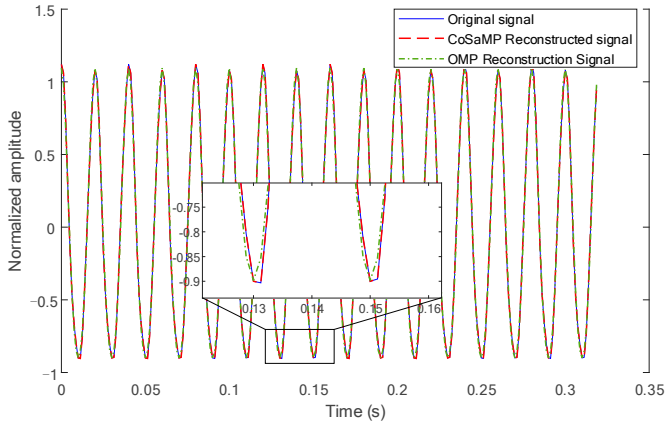

(**b**) 62 Hz supersynchronized oscillating signal

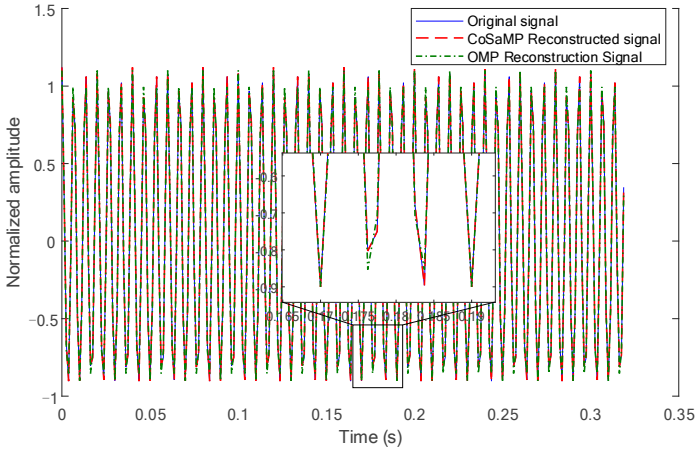

(**c**) 150 Hz medium to high frequency oscillating signals

Figure 11. Comparison of reconstruction algorithms in different oscillation bands.

4.2. Analysis of Model Training Results

The cross-entropy loss function is invoked before training to eliminate the effect of sample imbalance on the results, and the broadband oscillatory localization model composed of three layers of GAT, one fully connected layer, and a Softmax output layer is used for training; during the training process, the Epoch is set to be 60, the number of samples for each training is 80, the Learning Rate is set to be 0.001, and the Drop Rate is set to be 0.5; the training process is shown in Figure 8, and the formula for the accuracy rate is as follows:

$$I_{acc} = \frac{L}{L_N} \tag{17}$$

where: L is the number of samples correctly localized by the GAT network; L_N is the total number of test samples.

As can be seen in Figure 12, after 14 iterations, the whole training process begins to converge, and although training with compressed data cannot avoid errors with the original data, the loss rate is always in a decreasing trend during the training process, and the accuracy rate maintains a steady increase, indicating that the GAT model with multi-attention mechanism has a high accuracy rate combined with noise immunity.

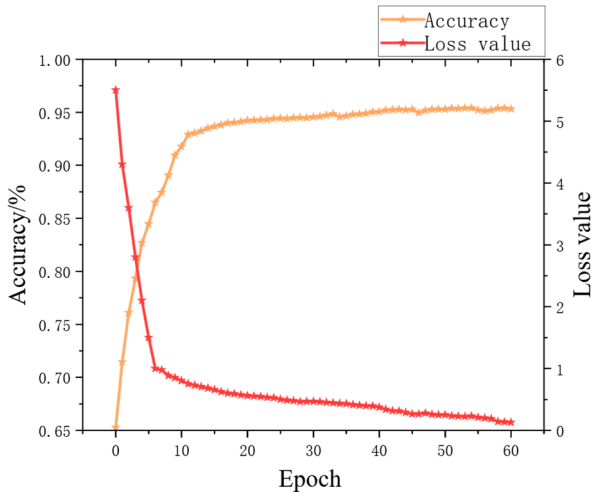

Figure 12. GAT training accuracy vs. loss rate.

4.3. Comparative Analysis of Model Performance

In order to better compare the superiority of GAT among other deep-learning models and to comprehensively and systematically test the performance of the wideband oscillation localization model, this paper introduces the confusion matrix shown in Table 2, which shows that, in addition to the conventional accuracy evaluation index A_C, the F_1 score also reflects the model's prediction ability for the oscillation samples.

Table 2. TSA confusion matrix.

Projected Value	Actual Value	
	Stabilization	**Destabilization**
Stabilization	T_p	F_p
Destabilization	F_N	T_N

The expression is as follows:

$$A_C = \frac{T_P + T_N}{T_P + T_N + F_P + F_N} \tag{18}$$

$$P_r = \frac{T_N}{T_N + F_N} \tag{19}$$

$$R_e = \frac{T_N}{T_N + F_P} \tag{20}$$

$$F_1 = \frac{2 \times P_r \times R_e}{P_r + R_e} \tag{21}$$

In this paper, CNN, GCN, and TCN replacing GAT are used to construct the broadband oscillation localization control model, respectively, and its parameter settings are shown in Table 3. Under the same arithmetic platform and sample conditions, the performance of each type of model is evaluated.

Table 3. Simulation operation conditions.

Mould	Parameterization
CNN	4-layer convolutional structure, convolutional kernel 3 × 3, learning rate 0.005, 80 iterations
GCN	4-layer convolutional structure, convolutional kernel as Chebyshev polynomials, learning rate 0.001, 64 iterations
TCN	Stacking 4 residual blocks, convolution kernel 3 × 3, and null coefficients of 1, 2, and 4

The performance of each model in the test set is shown in Figure 13.

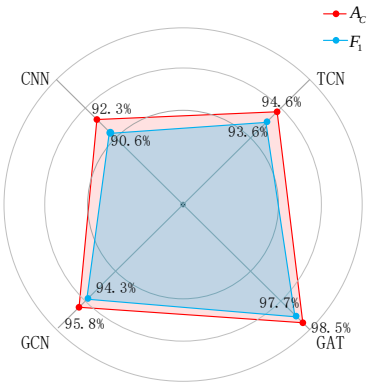

Figure 13. Comparison of the performance of the models.

From Figure 4, it can be clearly seen that the GAT algorithm with multi-attention mechanism has outstanding ability to learn topology and feature information in the TSA model, and the model accuracy is as high as 98.5%, which is 6.2% higher than the correct rate of the CNN model; and its omission rate and misjudgment rate have been significantly improved compared to the other models, which fully illustrates the effectiveness of the GAT algorithm proposed in this paper in the TSA model. The advantages of the algorithm proposed in this paper over other previous algorithms in the field can be clearly compared from Table 4.

Table 4. Comparison of success in the field.

Positioning Method	Applicable Oscillation Type	Methodological Features
Integrated learning	Negatively damped oscillations and forced power oscillations	The performance is good under both topology changes and measurement errors. There is still a need to consider how to further improve the performance through correlation analysis and feature selection.
Dempster-Shafer theory of evidence	Negatively damped oscillations and forced power oscillations	It is also possible to accurately localize forced oscillations that contain two sources of oscillation.
DTW and KNN based on Mahalanobis distance	Forced power oscillations	Higher robustness for unsynchronized data still requires further consideration of load-induced forced oscillations.

Table 4. *Cont.*

Positioning Method	Applicable Oscillation Type	Methodological Features
Deep migratory learning	Sub-synchronous oscillation	Deep learning is used for the first time to localize the subsynchronous oscillations with good noise immunity, and the performance in more complex wind farms is to be further studied.
Deep migratory learning	Forced power oscillations	Good localization of both noise content and recording incompleteness, as well as topology changes, needs to be explored for performance in larger systems.
Combination of compressed sensing and graphical attention networks	Forced power oscillations	Good localization effect for noise and incomplete recording, and good localization for topology change, which can be applied to all kinds of complex new power systems.

5. Conclusions

With the continuous penetration of a high percentage of new energy sources, the power system presents weak damping and is prone to broadband oscillations that threaten the safety of electricity. This study proposes a broadband oscillation localization model using the GAT algorithm, offering rapid and accurate localization of affected areas. The main conclusions are as follows.

The method utilizes the compressed perception technique to effectively downscale the high-dimensional broadband oscillatory signals, which not only helps the learning of graph neural networks, but also realizes high-precision signal reconstruction based on the low-dimensional signals. The error of the reconstructed signal is only 0.031, which fully proves that the compressed low-dimensional data can well characterize the information of the original high-dimensional signal. In addition, the method employs a multi-attention mechanism, which effectively captures the key information in the complex graph structure. By introducing the cross-entropy loss function, the effective treatment of unbalanced samples is realized, and the training accuracy of the model is enhanced to reach a high accuracy level of 98.5%. In addition, the scheme makes full use of the parallel computing capabilities of GPU and CPU; this reduces computation time significantly, enabling faster execution and more accurate node state identification. The results not only enhance localization accuracy, but also pave the way for future applications in smart grid systems.

On small or sparsely connected graphs, GAT may encounter overfitting problems. Because GAT is capable of learning very complex patterns, when there is insufficient training data, the model may overlearn the noise in the training set, which affects the generalization ability.

Author Contributions: Conceptualization, J.G. and Y.Y.; methodology, H.X. and J.G.; software, Y.X. and J.G.; validation, J.G., C.Z. and Y.Y.; formal analysis, Y.X. and J.G.; investigation, C.Z. and Y.Y.; resources, J.G. and H.D.; data curation, C.Z. and J.G.; writing—original draft preparation, H.X., J.G. and Y.Y.; writing—review and editing, J.G., H.X. and H.D.; visualization, Y.Y.; supervision, J.G. and H.D.; project administration, C.Z. and H.D.; funding acquisition, Y.Y. and H.D. All authors have read and agreed to the published version of the manuscript.

Funding: This research was funded by State Grid Corporation of China Science and Technology Program (522722240004).

Data Availability Statement: Readers who are interested in this study. Data can be obtained by contacting 11230951@stu.lzjtu.edu.cn.

Acknowledgments: Acknowledging the funding of this project from the Science and Technology Program of the State Grid Corporation Limited.

Conflicts of Interest: Author Honglei Xu was employed by the State Grid Gansu Electric Power Company. The authors declare that this study received funding from State Grid Corporation Limited. The funder was not involved in the study design, collection, analysis, interpretation of data, the writing of this article or the decision to submit it for publication. The remaining authors declare that the research was conducted in the absence of any commercial or financial relationships that could be construed as a potential conflict of interest.

References

1. Chen, W.; Wei, Z.; Zhen, W.; Yang, D.; Ping, J. Partition-based Network Equivalent Method for Power System Subsynchronous Oscillation Analysis. *J. Mod. Power Syst. Clean Energy* **2024**, *12*, 313–320.
2. Ma, W. Thoughts on the development of frontier technology in electrical engineering. *Trans. China Electrotech. Soc.* **2021**, *36*, 4627–4636.
3. Ma, N.; Xie, X.; He, J.; Wang, H. A review of broadband oscillations in power systems with a high proportion of new energy and power electronic devices. *Chin. J. Electr. Eng.* **2020**, *40*, 4720–4732.
4. Nong, L.; Ma, N.; Ding, M.; Hao, L.; Shi, B.; Xiao, X. New Power System Broadband Oscillation Prevention and Control System Architecture. *Grid Technol.* **2023**, *47*, 4092–4102.
5. Chen, L.; Xie, X.; He, J.; Xu, T.; Xu, D.; Ma, N. Wideband oscillation monitoring in power systems with high-penetration of renewable energy sources and power electronics: A review. *Renew. Sustain. Energy Rev.* **2023**, *175*, 113148. [CrossRef]
6. Ji, H.; Li, Y.; Ding, X.; Alghamdi, S.M.; Lu, J. Stability analysis of Boolean networks: An eigenvalue approach. *Appl. Math. Comput.* **2024**, *463*, 128361. [CrossRef]
7. Frutos, P.; Guerrero, J.M.; Muniategui, I.; Endemaño, A.; Ortega, D.; Briz, F. Low-frequency oscillations in AC railway traction power systems: Train input admittance calculation and stability analysis. *Int. J. Electr. Power Energy Syst.* **2024**, *162*, 110284. [CrossRef]
8. Liang, C.; Zuo, X.; Li, J.; Liu, R.; Huang, C. Stability analysis of doubly-fed fan with small disturbance oscillation based on regional decoupling impedance model. *Int. J. Electr. Power Energy Syst.* **2024**, *162*, 110236. [CrossRef]
9. Jin, B.; Yu, Y.; Fan, C.; Yi, W.; Ju, P. Tracing method of sub-/super-synchronous oscillation based on interharmonic power flow calculation of wide frequency measurement. *Electr. Power Auto Mation Equip.* **2022**, *42*, 221–228.
10. Liu, Z.; Yang, X.; Lv, X.; Chen, B.; Zhang, Y. Dynamic interaction analysis among different control loops and stability enhancement strategy for MMC-HVDC systems. *Int. J. Electr. Power Energy Syst.* **2023**, *147*, 108835. [CrossRef]
11. Hu, Y.; Bu, S.; Luo, J.; Wen, J. Generalization of oscillation loop and energy flow analysis for investigating various oscillations of renewable energy systems. *Renew. Energy* **2023**, *218*, 119352. [CrossRef]
12. Mohd, Z.; Mohd, R.; Mohd, T. A novel method for locating the source of sustained oscillation in power system using synchrophasors data. *Prot. Control. Mod. Power Syst.* **2020**, *5*, 1–12.
13. Yan, X.; Zheng, G.; Kai, S. Location and Mechanism Analysis of Oscillation Source in Power Plant. *IEEE Access* **2020**, *8*, 97452–97461.
14. Ren, Y.; Chen, L.; Min, Y.; Li, Y. Relationship between transient energy flow, electric power and damping torque in subsynchronous oscillation. *Autom. Electr. Power Syst.* **2018**, *42*, 52–58.
15. Chen, L.; Wang, W.; Wang, M.; Min, Y. Disturbance source location of subsynchronous forced oscillation and damping evaluation using transient energy flow. *Autom. Electr. Power Syst.* **2016**, *40*, 1–8.
16. He, J.; Luo, G.; Cheng, M. A Research Review on Application of Artificial Intelligence in Power System Fault Analysis and Location. *Proc. Chin. Soc. Electr. Eng.* **2020**, *40*, 5506–5515.
17. Liu, D.; Zhang, D.; Sun, H.; Ma, S. Construction of stability situation quantitative assessment and adaptive control system for large-scale power grid in the spatio-temporal big data environment. *Proc. Chin. Soc. Electr. Eng.* **2015**, *35*, 268–276.
18. Feng, S.; Cui, H.; Wu, X.; Feng, J.; Zou, C.; Zhao, X.; Tang, Y. Monitoring method of wide-band oscillation based on compressed sensing of diagonalizable LDPC and k-nearest neighbour algorithm. *Power Syst. Technol.* **2021**, *45*, 3025–3033.
19. Cui, H.; Feng, S.; Chen, J.; Ye, Y. Wide-area location method of wide-band oscillations based on autoencoder and Long Short-term Memory network. *Autom. Electr. Power Syst.* **2022**, *46*, 194–201.
20. Wu, Y.; Yao, J.; Chang, N.; Zhang, Q.; Fan, C.; Dou, R. Design and implementation of multi-functional wide-frequency measurement device. *Autom. Electr. Power Syst.* **2020**, *44*, 136–141.
21. Zhang, C.; Xue, S.; Li, J.; Wu, J.; Du, B.; Liu, D.; Chang, J. Multi-Aspect enhanced Graph Neural Networks for recommendation. *Neural Netw.* **2023**, *157*, 90–102. [CrossRef] [PubMed]
22. Wang, X.; Ji, H.; Shi, C.; Wang, B.; Ye, Y.; Cui, P.; Yu, P.S. Heterogeneous graph attention network. In Proceedings of the World Wide Web Conference, San Francisco, CA, USA, 13–17 May 2019; pp. 2022–2032.

23. Wu, H.; Xu, Z. Multi-energy flow calculation in integrated energy system via topological graph attention convolutional network with transfer learning. *Energy* **2024**, *303*, 132018. [CrossRef]
24. Zhang, J.; Guo, L.; Wang, G.; Yu, J.; Zheng, X.; Mei, Y.; Han, B. A dual-level graph attention network and transformer for enhanced trajectory prediction under road network constraints. *Expert Syst. Appl.* **2025**, *261*, 125510. [CrossRef]
25. Xie, Z.; Liu, L.; Chen, Z. Image compressed sensing: From deep learning to adaptive learning. *Knowl.-Based Syst.* **2024**, *293*, 111659. [CrossRef]
26. Ding, H.; Zhao, H.; Liu, J.; Ren, M.; Dai, R. Power equipment state sensing technology based on compressed sensing. *High Volt. Eng.* **2020**, *46*, 1877–1885.
27. Shao, M.; Wu, J.; Li, B.; Zhang, R. Transient stability assessment of power system based on two-stage ensemble deep belief network. *Power Syst. Technol.* **2020**, *44*, 1776–1787.

Disclaimer/Publisher's Note: The statements, opinions and data contained in all publications are solely those of the individual author(s) and contributor(s) and not of MDPI and/or the editor(s). MDPI and/or the editor(s) disclaim responsibility for any injury to people or property resulting from any ideas, methods, instructions or products referred to in the content.